

Borromean Feshbach resonance in ^{11}Li studied via $^{11}\text{Li}(p,p')$

Takuma Matsumoto,^{1,*} Junki Tanaka,^{2,3,4} and Kazuyuki Ogata²

¹*Department of Physics, Kyushu University, Fukuoka 819-0395, Japan*

²*Research Center for Nuclear Physics, Osaka University, Ibaraki, Osaka 567-0047, Japan*

³*Department of Physics, Konan University, Higashinada, Kobe, Hyogo 658-8501, Japan*

⁴*Institut für Kernphysik, Technische Universität Darmstadt, 64289 Darmstadt, Germany*

(Dated: October 15, 2018)

A dipole resonance of ^{11}Li is newly found by a $^9\text{Li} + n + n$ three-body model analysis with the complex-scaling method. The resonance can be interpreted as a bound state in the $^{10}\text{Li} + n$ system, that is, a Feshbach resonance in the $^9\text{Li} + n + n$ system. As a characteristic feature of the Feshbach resonance of ^{11}Li , the $^{10}\text{Li} + n$ threshold is open above the $^9\text{Li} + n + n$ one, which reflects a distinctive property of the Borromean system. A microscopic four-body reaction calculation for the $^{11}\text{Li}(p,p')$ reaction at 6 MeV/nucleon is performed by taking into account the resonance and nonresonant continuum states of the three-body system. The angular distribution of the elastic and inelastic scattering as well as the breakup energy spectrum recently observed are reproduced well.

Elucidation of resonances, which are omnipresent in different hierarchies in nature, is one of the most important subjects in physics. For example, the tetraquark and pentaquark baryons in hadron physics [1] as well as the so-called Efimov resonance [2, 3] of ultracold atoms in atomic physics have attracted the attention of many experimentalists and theorists. In nuclear physics, various resonances have been discovered and investigated in detail. Studies of resonances in nuclear physics will be characterized by the diversity. Nuclei, a self-organized strongly interacting system, show a wide variety of structures as the atomic number, the mass number, and the excitation energy change. From a different point of view, we have better knowledge on the basic interaction that forms many-nucleon systems than in hadron physics. Various types of resonances, e.g., single-particle resonances, gas-like α cluster states, and giant resonances have therefore been investigated on the solid basis. Nowadays resonant structures for nuclei near and even beyond the neutron dripline have intensively been proceeded. Furthermore, a recent experiment suggested that four neutrons form a resonance, that is, the so-called tetra-neutron [4].

Some nuclei near the dripline such as ^6He , ^{11}Li , ^{14}Be , and ^{22}C are known as two-neutron halo nuclei [5–8] consisting of a core nucleus and two loosely bound neutrons. These nuclei have a Borromean structure, meaning that there is no bound state for each pair of the three constituents. Except for ^6He , experimental information on resonances of such Borromean nuclei is very scarce. Existence of a resonance of ^{11}Li , the firstly discovered Borromean nucleus, is a longstanding open question in particular [9–22].

Very recently, measurement of the $^{11}\text{Li}(p,p')$ reaction at 6 MeV/nucleon with a high statistic and high resolution has been performed [23], and a low-lying excited state of ^{11}Li has clearly been identified. In the analysis, the authors adopted a macroscopic model for the transition of ^{11}Li combined with the distorted wave Born approximation (DWBA); a form factor of the isoscalar electric dipole ($E1$) excitation is assumed. The macroscopic model, however, does not describe the Borromean nature of ^{11}Li and a microscopic approach to the structure of the low-lying continuum states of ^{11}Li is eagerly

desired. On the reaction side, the applicability of DWBA in the energy region of our interest is quite questionable. In other words, if the reaction observable *suffers* from higher-order processes, it is not trivial at all to relate the observable and a response of a nucleus to a specific transition operator. Furthermore, there is no guarantee that a single operator is responsible for the proton inelastic scattering measured at backward angles. The purpose of this Letter is to analyze the $^{11}\text{Li}(p,p')$ cross sections at 6 MeV/nucleon with a sophisticated reaction model, that is, the microscopic four-body continuum-discretized coupled-channels method (CDCC) [24–28]. A complete set of the $^9\text{Li} + n + n$ three-body wave functions in a space relevant to the $^{11}\text{Li}(p,p')$ reaction is implemented in CDCC and thereby the validity of the continuum structure of ^{11}Li is examined. Classification of the three-body wave functions with the complex-scaling method (CSM) [29–31] suggests a low-lying three-body Feshbach resonance [32] of ^{11}Li , which is the principal finding of the present study.

For ^{11}Li , we adopt a $^9\text{Li} + n + n$ three-body model, with assuming for simplicity that ^9Li is a spinless and inert particle that has a naïve shell-model configuration. This simplified model has been applied to analyses of some reactions of ^{11}Li [15–17]. Three-body wave functions $\Phi_{I^\pi\nu}$, where I^π represents the spin-parity and ν is the index of eigenenergy, of ^{11}Li are obtained by diagonalizing the three-body Hamiltonian:

$$h = K_r + K_y + V_{nn} + V_{cn} + V_{cn} + V_{cnn}. \quad (1)$$

Here, K_r and K_y are the kinetic energy operators for the Jacobi coordinates \mathbf{r} and \mathbf{y} shown in Fig. 1 in Ref. [25], respectively. V_{nn} (V_{cn}) is a two-body interaction between the two neutrons (^9Li and a neutron), and V_{cnn} is a phenomenological three-body force (3BF). $\Phi_{I^\pi\nu}$ is explicitly antisymmetrized for the exchange between the two valence neutrons, whereas the exchange between each valence neutron and a nucleon in ^9Li is approximately treated by the orthogonality condition model [33].

For understanding properties of the three-body continuum of ^{11}Li in more detail, we employ CSM, in which the radial

part of each Jacobi coordinate is transformed as

$$r \rightarrow r e^{i\theta_c}, \quad y \rightarrow y e^{i\theta_c} \quad (2)$$

with the scaling angle θ_c , and h is rewritten as h^{θ_c} accordingly. As a result of diagonalization of h^{θ_c} , eigenstates $\varphi_{I^\pi\nu}^{\theta_c}$ that have complex eigenenergies $\varepsilon_{I^\pi\nu}^{\theta_c}$ are obtained. A resonance is identified as an eigenstate on the complex-energy plane isolated from other nonresonant states; the real and imaginary parts of the eigenenergy represent the resonant energy ε_R and a half of the decay width $\Gamma/2$, respectively.

The total wave function Ψ of the $p + {}^{11}\text{Li}$ reaction system is obtained by solving the Schrödinger equation

$$\left(K_R + h + \sum_{i \in {}^{11}\text{Li}} v_{0i} + V_C - E \right) \Psi^{(+)} = 0, \quad (3)$$

where K_R is the kinetic energy operator regarding the coordinate \mathbf{R} between the center-of-mass of ${}^{11}\text{Li}$ and p . The nuclear interaction between p and the i th nucleon in ${}^{11}\text{Li}$ is denoted by v_{0i} . V_C is the Coulomb interaction between p and the center-of-mass of ${}^{11}\text{Li}$; we thus ignore the Coulomb breakup process.

In CDCC, $\Psi^{(+)}$ is approximately expanded in terms of a finite number of $\Phi_{I^\pi\nu}$ as

$$\Psi^{(+)} \approx \sum_{\gamma} \chi_{\gamma}^{(+)}(\mathbf{R}) \Phi_{I^\pi\nu}, \quad (4)$$

where $\gamma = (I^\pi, \nu)$ and $\chi_{\gamma}^{(+)}$ is the relative wave function regarding \mathbf{R} . Inserting Eq. (4) into Eq. (3) leads to a set of coupled equations for $\chi_{\gamma}^{(+)}$:

$$\begin{aligned} [K_R + U_{\gamma\gamma}(\mathbf{R}) - (E - \varepsilon_{\gamma})] \chi_{\gamma}^{(+)}(\mathbf{R}) \\ = - \sum_{\gamma' \neq \gamma} U_{\gamma\gamma'}(\mathbf{R}) \chi_{\gamma'}^{(+)}(\mathbf{R}) \end{aligned} \quad (5)$$

with $\varepsilon_{\gamma} = \langle \Phi_{I^\pi\nu} | h | \Phi_{I^\pi\nu} \rangle$. For coupling potentials $U_{\gamma'\gamma}$, we adopt a microscopic folding model [40–42] with transition densities of ${}^{11}\text{Li}$ for 11 nucleons, which can be calculated with $\Phi_{I^\pi\nu}$ and a ground state density of ${}^9\text{Li}$ for 9 nucleons [16]. Equation (5) is solved under the standard boundary condition; details are shown in Ref. [24].

By solving Eq. (5), one obtains a transition matrix element from which a cross section to the ground state or a discretized-continuum state of ${}^{11}\text{Li}$ can be evaluated. To obtain a continuous breakup energy spectrum, we employ the smoothing method based on CSM proposed in Ref. [28]. Consequently, the double differential breakup cross section with respect to the energy ε of the ${}^9\text{Li} + n + n$ system measured from the three-body threshold and the solid angle Ω of the center-of-mass of the three particles, $d^2\sigma/(d\varepsilon d\Omega)$, is obtained. As shown by Eq. (21) in Ref. [28], the breakup energy spectrum is given by an incoherent sum of the contributions from the eigenstates of h^{θ_c} . This property is crucial to clarify the role of a resonance in describing breakup observables.

As for the numerical input, we take the Minnesota force [34] for V_{nn} and the interaction used in Ref. [35] is

adopted as V_{cn} . The V_{cn} generates a resonance of ${}^{10}\text{Li}$ in the $0p_{1/2}$ state with the resonant energy (decay width) of 0.46 MeV (0.36 MeV). This resonance is denoted by ${}^{10}\text{Li}$ below for simplicity. This value of the resonant energy is in good agreement with the latest experimental data [36]. For V_{cnn} , we adopt the volume-type 3BF [37] given by a product of Gaussian functions for the two Jacobi coordinates; the range parameter for each coordinate is set to 2.64 fm and the strength is determined to optimize the ground state energy $\varepsilon_0 = -0.369$ MeV [38] of ${}^{11}\text{Li}$. We employ the Jeukennd-Lejeune-Mahaux (JLM) effective nucleon-nucleon interaction [39] as v_{0i} . As in the preceding works [40–42], a normalization factor N_I for the imaginary part of the JLM interaction is introduced; N_I is determined to be 0.55 so as to reproduce both the elastic and breakup cross section data around 100° , where the breakup cross section data exist. Note that we do not include any other adjustable parameters. Eigenstates of h and h^{θ_c} are obtained by the Gaussian expansion method (GEM) [43], where we adopt the parameter set II for h and set III for h^{θ_c} shown in Table I in Ref. [28]. In CSM, the scaling angle θ_c is set to 20° . In CDCC calculation, we select the $\Phi_{I^\pi\nu}$ with $\varepsilon < 5$ MeV and the resulting number of states is 93, 111, and 131 for $I^\pi = 0^+$, 1^- , and 2^+ , respectively. The model space gives good convergence of the elastic and breakup cross sections.

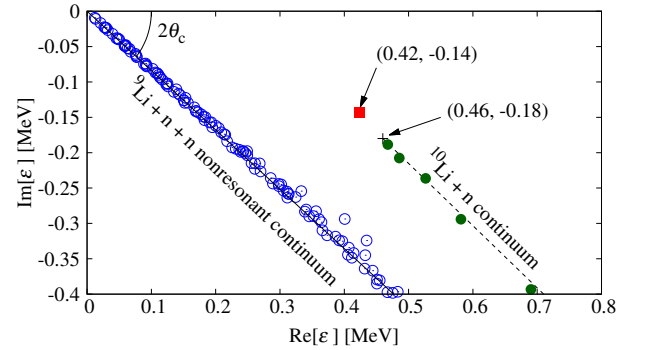


FIG. 1: Eigenenergies for 1^- states calculated with CSM on the complex-energy plane measured from the ${}^9\text{Li} + n + n$ threshold. The scaling angle θ_c is taken to be 20° , and the cross mark shows the ${}^{10}\text{Li}-n$ threshold on the complex plane.

We first discuss the structure of the continuum states of ${}^{11}\text{Li}$ (the ${}^9\text{Li} + n + n$ system). For this purpose in Fig. 1 we plot the eigenenergies of h^{θ_c} with $I^\pi = 1^-$ on the complex-energy plane. The solid square represents the three-body resonance of ${}^{11}\text{Li}$ with $\varepsilon_R = 0.42$ MeV and $\Gamma/2 = 0.14$ MeV, where ε_R is consistent with the value obtained in Ref. [18]. The open circles represent three-body nonresonant continuum states of the ${}^9\text{Li} + n + n$ system, whereas the closed circles indicate two-body continuum states between the valence neutron and ${}^{10}\text{Li}$. One may find that the three-body resonance is located near the ${}^{10}\text{Li}-n$ threshold and the energy of the valence neutron is negative with respect to ${}^{10}\text{Li}$. This indicates that the dipole resonance of ${}^{11}\text{Li}$ is a Feshbach resonance [32] in a

three-body system. We will return to this point later.

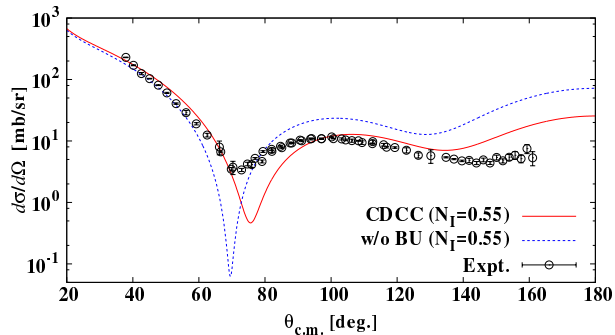


FIG. 2: Angular distribution of the differential elastic cross section for the $^{11}\text{Li} + p$ scattering at 6 MeV/nucleon [23]. The solid and dotted lines represent results of the microscopic four-body CDCC and without breakup channels, respectively.

Next we discuss how the continuum structure of ^{11}Li affects reaction observables. Figure 2 shows the angular distribution of the elastic scattering of ^{11}Li on p at 6 MeV/nucleon. The solid and dotted lines show the results with and without breakup effects; the former corresponds to the microscopic four-body CDCC calculation. The solid line which is adjusted to the data around 100° with setting $N_I = 0.55$, agree well with the data at forward angles. One can see that breakup effects represented by the difference between the dotted and solid lines are significant for the elastic scattering. The solid line deviates from the data around the dip of the cross section. It is known that in the region a spin-orbit part of the distorting potential, which is disregarded in the present study, plays an important role. It should be noted also that the JLM is applicable to nucleon scattering above 10 MeV [39]. Considering these things, we conclude that the agreement between the solid line and the experimental data is satisfactory.

In Fig. 3(a) we show the angular distribution of the breakup cross section; $d^2\sigma/(d\epsilon d\Omega)$ is integrated over ϵ from 0 MeV to 1.13 MeV so as to cover well the peak structure of the cross section in Fig. 3(b). The thick solid line represents the result of the microscopic four-body CDCC; it reproduces the experimental data around 100° , as N_I is chosen so. The slight deviation of the solid line from the data around 80° will come from the same reason as for the elastic cross section. The dotted, dashed and dot-dashed lines represent the breakup cross sections to the 0^+ , 1^- and 2^+ states, respectively. One sees that the breakup cross section to the 1^- state is dominant but the 0^+ and 2^+ components are not negligible in the region where the experimental data exist. In other words, a model that assumes a pure dipole transition of ^{11}Li will not explain the measured cross sections unless an unrealistic structural model of ^{11}Li is adopted. Furthermore, since the transition potential adopted in the present calculation cannot be written as a simple functional form, to use a single transition operator can not be justified. Our final remark on Fig. 3(a) is the importance of the coupled-channel effects. The thin solid line

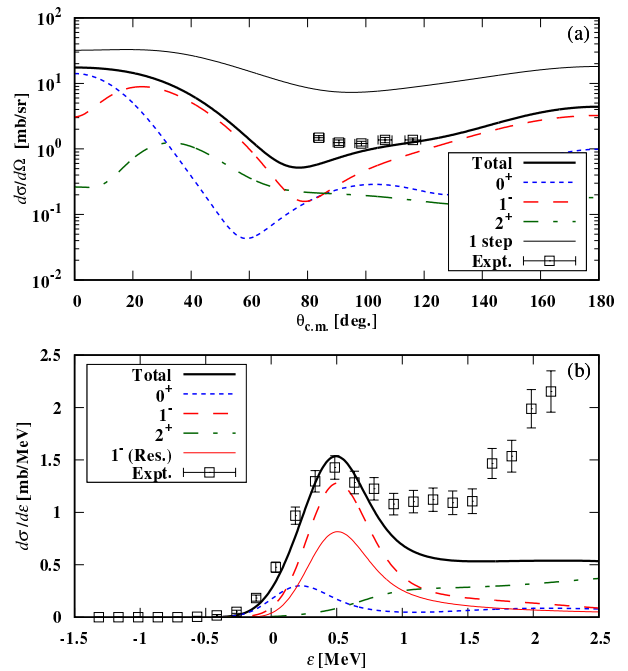


FIG. 3: (a) Angular distribution of the differential breakup cross section and (b) the breakup cross section as a function of the three-body breakup energy ϵ of ^{11}Li in the $^{11}\text{Li}(p, p')$ reaction [23]. The cross section in (a) is obtained by integrating $d^2\sigma/(d\epsilon d\Omega)$ over ϵ from 0 MeV to 1.13 MeV, and that in (b) over $\theta_{c.m.}$ from 115° to 124° . The dotted, dashed, and dot-dashed lines represent calculated cross sections to the 0^+ , 1^- , and 2^+ breakup states, respectively, and the sum of them is shown by the thick solid line. The thin solid line shows the total cross section calculated with a one-step approximation in panel (a) and the contribution of the three-body resonance of ^{11}Li in panel (b).

shows the result of a one-step calculation that severely overestimates the thick solid line by about one-order at middle angles. We therefore conclude that DWBA is not applicable to the $^{11}\text{Li}(p, p')$ at 6 MeV/nucleon.

In Fig. 3(b), we show the breakup cross section with respect to the three-body energy ϵ after breakup, which is obtained by integrating $d^2\sigma/(d\epsilon d\Omega)$ over $\theta_{c.m.}$ from 115° to 124° . Here, we have taken into account the energy resolution of the experimental data. The total breakup cross section represented by the thick solid line reproduces the experimental data up to $\epsilon \sim 1.0$ MeV including a low-lying peak. One sees that the contribution from the dipole resonance of ^{11}Li shown by the thin solid line dominates the low-lying peak. Although the calculated resonant width $\Gamma = 0.28$ MeV is narrow compared with the evaluation $\Gamma = 1.15 \pm 0.06$ MeV in Ref. [23], the measured $d\sigma/d\epsilon$ spectrum is reproduced by taking into account the 0^+ and 2^+ non-resonant components. It can be concluded therefore that the nonresonant components should be properly evaluated and subtracted from the measured spectrum to extract reliable information on the resonance. The calculated cross section undershoots the data for $\epsilon \gtrsim 1.0$ MeV, which will be due to some other degrees of freedom that are

not taken into account in the present calculation, for example, a transition to higher spin states and a core excitation in ${}^9\text{Li}$.

Thus we have shown through CDCC calculation that the three-body structure of ${}^{11}\text{Li}$ both in the bound and continuum states including the dipole resonance of ${}^{11}\text{Li}$ shown in Fig. 1 is consistent with the measured cross sections. We here discuss the property of the ${}^{11}\text{Li}$ resonance. As mentioned above, the resonance is located near the ${}^{10}\text{Li}-n$ threshold. A certain connection between the ${}^{11}\text{Li}$ resonance and ${}^{10}\text{Li}$ is therefore expected, as suggested in Ref. [18]. To clarify this, we change the strength of V_{cn} with multiplied by λ_{nc} and see the positions of the two resonances on the complex-energy plane; the result is shown in Table I. One sees that the ${}^{11}\text{Li}$ resonance, if exists, always shows up near the ${}^{10}\text{Li}-n$ threshold. For λ_{nc} less than 0.96, the resonant pole of ${}^{11}\text{Li}$ cannot be found clearly. The property of the ${}^{11}\text{Li}$ resonance thus strongly depends on that of ${}^{10}\text{Li}$, and ε_R of ${}^{11}\text{Li}$ is always below ε_R of ${}^{10}\text{Li}$.

λ_{nc}	${}^{10}\text{Li} (\varepsilon_R, -\Gamma/2)$	${}^{11}\text{Li} (\varepsilon_R, -\Gamma/2)$
1.00	(0.46, -0.18)	(0.42, -0.14)
0.99	(0.51, -0.21)	(0.49, -0.18)
0.98	(0.55, -0.24)	(0.54, -0.23)
0.97	(0.60, -0.28)	(0.59, -0.27)
0.96	(0.65, -0.32)	-

TABLE I: Calculated resonant energies (ε_R) and widths (Γ) of ${}^{10}\text{Li}$ and ${}^{11}\text{Li}$ in the unit of MeV. λ_{nc} is a scaling factor of V_{cn} .

Moreover, to investigate the existence probability of ${}^{10}\text{Li}$ in ${}^{11}\text{Li}$ continuum states, we calculate an overlap function between $\varphi_{1^-n}^{\theta_c}$ and a complex-scaled wave function of ${}^{10}\text{Li}$, $\phi_{\frac{1}{2}^-}^{\theta_c}$, defined by

$$\alpha_n^{\theta_c} = 2 \langle \tilde{\varphi}_{1^-n}^{\theta_c} | \phi_{\frac{1}{2}^-}^{\theta_c} \rangle \langle \tilde{\varphi}_{\frac{1}{2}^-}^{\theta_c} | \varphi_{1^-n}^{\theta_c} \rangle, \quad (6)$$

where a factor of 2 means to exist two pairs of the ${}^9\text{Li}-n$ system in ${}^{11}\text{Li}$. In general, $\alpha_n^{\theta_c}$ becomes complex, and its real part can be interpreted as a probability [44]. In fact, for the ${}^9\text{Li}+n+n$ nonresonant continuum states shown by the open circles in Fig. 1, which are expected not to contain ${}^{10}\text{Li}$, the real part of $\alpha_n^{\theta_c}$ is almost 0. On the other hand, the real part of $\alpha_n^{\theta_c}$ is larger than 0.9 for the ${}^{10}\text{Li}+n$ continuum states shown by the closed circles in Fig. 1. For the ${}^{11}\text{Li}$ resonance, the real part of $\alpha_n^{\theta_c}$ exceeds 0.9 as the ${}^{10}\text{Li}+n$ continuum states. It should be noted that since ε_R of ${}^{10}\text{Li}$ is higher than ε_R of the ${}^{11}\text{Li}$ resonance, one can interpret that the ${}^{11}\text{Li}$ resonance is a bound state of the ${}^{10}\text{Li}+n$ system. The ${}^{10}\text{Li}-n$ relative wave function can be regarded as an s -wave because I^π of the ${}^{11}\text{Li}$ resonance is 1^- and that of ${}^{10}\text{Li}$ is $1/2^-$. From the point of view of a bound state embedded in the ${}^9\text{Li}+n+n$ three-body continuum, the ${}^{11}\text{Li}$ resonance can be interpreted as a Feshbach resonance [32]. In Fig. 4, we summarize properties of the complex-scaled states shown in Fig. 1. In the three-body Feshbach resonance, the ${}^9\text{Li}+n+n$ threshold energy is lower

than the ${}^{10}\text{Li}-n$ threshold, which is a distinctive character of the Borromean system. We thus refer to this resonance as a *Borromean Feshbach resonance*.

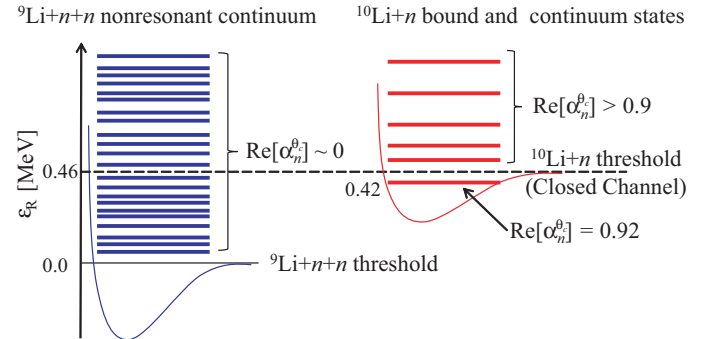


FIG. 4: A schematic representation of complex-scaled states of ${}^{11}\text{Li}$ for $I^\pi = 1^-$ is shown.

In conclusion, we have found a dipole resonance in ${}^{11}\text{Li}$ at 0.42 MeV with the width of 0.28 MeV in a ${}^9\text{Li}+n+n$ three-body model calculation with CSM. The continuum structure of the three-body system including the resonance has been validated by the good agreement between the results of the microscopic four-body CDCC calculation and the recently measured ${}^{11}\text{Li}(p, p')$ data at 6 MeV/nucleon for both the angular distribution and the breakup energy spectrum. Important remarks on the comparison with the experimental data are i) contribution of not only the resonance but also the nonresonant continuum states are important, ii) a one-step calculation (DWBA) does not work at all, and iii) the transition operator cannot be written in a simple form as assumed in preceding studies.

The ${}^{11}\text{Li}$ resonance is interpreted as a bound state of the valence neutron with respect to ${}^{10}\text{Li}$, that is, a Borromean Feshbach resonance. It should be noted that the ${}^{10}\text{Li}-n$ threshold is above the ${}^9\text{Li}+n+n$ three-body threshold, which is a distinctive character of a Borromean system. The ordinary Feshbach resonance has intensively been discussed mainly in atomic physics. The finding of the Borromean Feshbach resonance in the present study will be characterized by its appearance in a Borromean system that is unique in the nucleonic system. Another important feature is that we have some pieces of information on the interactions between the constituents of ${}^{11}\text{Li}$. This allows one to carry out realistic studies on the ${}^{11}\text{Li}$ resonance. Nevertheless, more information on the n - ${}^9\text{Li}$ interaction will be desired to make our understanding on the continuum structure of ${}^{11}\text{Li}$ more profound and complete. Inclusion of the intrinsic spin of ${}^9\text{Li}$ as well as the excitation of the ${}^9\text{Li}$ core will also be very important.

Acknowledgments

The authors are grateful to Prof. I. Tanihata and Prof. N. Aoi for fruitful discussions. J.T. gratefully acknowledges

the support by the Hirao Taro Foundation of the Konan University Association for Academic Research. This work has been supported in part by Grants-in-Aid of the Japan Society for the Promotion of Science (Grants No. JP16K05352).

* matsumoto@phys.kyushu-u.ac.jp

- [1] H. X. Chen *et al.*, Phys. Rep. **639**, 1 (2016).
- [2] V. Fums, Phys. Lett. **33B**, 563 (1970).
- [3] B. Huang *et al.*, Phys. Rev. Lett. **112**, 190401 (2014).
- [4] K. Kisamori *et al.*, Phys. Rev. Lett. **116**, 052501 (2016).
- [5] I. Tanihata *et al.*, Phys. Rev. Lett. **55**, 2676 (1985); Phys. Lett. **B206**, 592 (1988).
- [6] T. Suzuki *et al.*, Nucl. Phys. **A658**, 313 (1999).
- [7] T. Moriguchi *et al.*, Nucl. Phys. **A929**, 83 (2014).
- [8] K. Tanaka *et al.*, Phys. Rev. Lett. **104**, 062701 (2010).
- [9] K. Ieki *et al.*, Phys. Rev. Lett. **70**, 730 (1993); D. Sackett *et al.*, Phys. Rev. C **48**, 118 (1993).
- [10] S. Shimoura *et al.*, Phys. Lett. B **348**, 29 (1995).
- [11] M. Zinser *et al.*, Nucl. Phys. **A619**, 151 (1997).
- [12] T. Nakamura *et al.*, Phys. Rev. Lett. **96**, 252502 (2006).
- [13] A. A. Korshennikov *et al.*, Phys. Rev. **C53**, R537 (1997).
- [14] A. A. Korshennikov *et al.*, Phys. Rev. Lett. **78**, 2317 (1997).
- [15] R. Crespo *et al.*, Phys. Rev. C **66**, 021002(R) (2002).
- [16] S. N. Ershov *et al.*, Phys. Rev. C **70**, 054608 (2004).
- [17] E. C. Pinilla *et al.*, Phys. Rev. C **85**, 054610 (2012).
- [18] E. Garrido *et al.*, Nucl. Phys. **A722**, 221c (2003).
- [19] K. Hagino and H. Sagawa, Phys. Rev. **C72**, 044321 (2005).
- [20] T. Myo *et al.*, Prog. Theor. Phys. **119**, 561 (2008).
- [21] Y. Kikuchi *et al.*, Phys. Rev. **C87**, 034606 (2013).
- [22] R. Kanungo *et al.*, Phys. Rev. Lett. **114**, 192502 (2015).
- [23] J. Tanaka *et al.*, accepted to Phys. Lett. B, arXiv:1708.07719.
- [24] M. Yahiro *et al.*, Prog. Theor. Exp. Phys. **2012**, 01A206 (2012).
- [25] T. Matsumoto, *et al.*, Phys. Rev. C **70**, 061601(R) (2004).
- [26] T. Matsumoto, *et al.*, Phys. Rev. C **73**, 051602(R) (2006).
- [27] M. Rodríguez-Gallardo, *et al.*, Phys. Rev. C **77**, 064609 (2008).
- [28] T. Matsumoto *et al.*, Phys. Rev. C **82**, 051602 (2010).
- [29] J. Aguilar and J.M. Combes, Commun. Math. Phys. **22**, 269 (1971).
- [30] E. Balslev and J.M. Combes, Commun. Math. Phys. **22**, 280 (1971).
- [31] S. Aoyama *et al.*, Prog. Theor. Phys. **116**, 1 (2006).
- [32] H. Feshbach, Ann. Phys. (N.Y.) **5**, 357 (1958); **19**, 287 (1962).
- [33] S. Saito, Prog. Theor. Phys. **41** (1969), 705.
- [34] D. R. Thompson *et al.*, Nucl. Phys. **A286**, 53 (1977).
- [35] H. Esbensen and G. F. Bertsch, Nucl. Phys. A **542**, 310 (1992).
- [36] M. Cavallaro *et al.*, Phys. Rev. Lett. **118**, 012701 (2017).
- [37] T. Matsumoto and M. Yahiro, Phys. Rev. **C90**, 041602(R) (2014).
- [38] M. Smith *et al.*, Phys. Rev. Lett. **101**, 202501 (2008).
- [39] J.-P. Jeukenne *et al.*, Phys. Rev. C **16**, 80 (1977).
- [40] T. Matsumoto *et al.*, Phys. Rev. C **83**, 064611 (2011).
- [41] D. Ichinkhorloo Phys. Rev. C **86**, 064604 (2012).
- [42] H. Guo *et al.*, Phys. Rev. C **87**, 024610 (2013).
- [43] E. Hiyama *et al.*, Prog. Part. Nucl. Phys. **51**, 223 (2003).
- [44] C. Kurokawa and K. Katō, Nucl. Phys. A **792**, 87 (2007).